Testing Functional Brain Activation and Connectivity for Visual Attention Processing between Young Adults with Primary Attention-Deficit/Hyperactivity Disorder (ADHD) and Traumatic Brain Injury (TBI) using Functional Near-Infrared Spectroscopy (fNIRS)

Jerry Shih-Ming Wang[1], Ziyan Wu[2], Yuyang Luo[3], Xiaobo Li, Ph.D.[4]

1. Undergraduate student researcher, Department of Electrical and Computer Engineering, Cockrell School of Engineering, The University of Texas at Austin.

2. Ph.D. Candidate, Computational Neuroanatomy and Neuroinformatics Lab, Department of Biomedical Engineering, Newark College of Engineering, New Jersey Institute of Technology.

3. Ph.D. Candidate, Computational Neuroanatomy and Neuroinformatics Lab, Department of Biomedical Engineering, Newark College of Engineering, New Jersey Institute of Technology.

4. Principal Investigator, Computational Neuroanatomy and Neuroinformatics Lab, Department of Biomedical Engineering, Newark College of Engineering, New Jersey Institute of Technology.

Abstract

Objective— The neurobiological mechanisms of inattention in people with primary attention-deficit/hyperactivity disorder (ADHD) and people post traumatic brain injury (TBI) are not yet well understood. Altered functional brain activations in the prefrontal, frontal, and parietal cortices have been reported in primary ADHD; secondary ADHD has been reported for people with different regional damages post TBI in some longitudinal studies. The objective of this study was to test the hypothesis that young adults with ADHD have significant differences in their functional brain regions of interest (ROI) activations and between-ROI connectivity patterns as compared to those with TBI, and that these functional alterations would be related to their respective inattentive symptoms of the disorders.

Method— Visual attention processing task-based functional near-infrared spectroscopy data from three demographically matched groups were analyzed: 20 subjects with predominantly inattention and/or combined symptoms on Conners' Adult ADHD Rating Scales (CAARS) for ADHD, 20 subjects with mild or moderate scale on Glasgow coma scale (GCS) for TBI, and 19 normal control subjects. Cortical activation maps for ROIs and between-ROI connectivity patterns were created for individual participants. Significant differences among the three groups of brain activation and connectivity were determined using one-way analysis of variance (one-way ANOVA) and one-way analysis of covariance (one-way ANCOVA), and significant between-group differences were determined using Tukey's honest significance difference test (Tukey's HSD).

Results— Compared to controls, subjects with TBI have significantly increased activation in the right calcarine gyrus (CG), significantly decreased connectivity between left middle frontal gyrus (MFG) and right CG, and significantly increased connectivity between right CG and right inferior occipital cortex (IOC). Compared to controls, subjects with primary

ADHD have significantly increased connectivity between left CG and right IOC. In addition, compared to TBI group, subjects with primary ADHD have significant higher connectivity between left MFG and right CG when covariates, age and gender, were regressed out.

Conclusion— The current data suggests that there are abnormal brain activation in right CG and significantly increased connectivities between left MFG and right CG, left CG and right IOC, and left IOC and right IOC that may play an important role in inattention for young adults with primary ADHD and young adults with TBI. Age and/or gender did not have a significant effect on the ROI activations and between-ROI connectivities in this study. It did have an effect on the connectivity between left MFG and right CG, albeit insignificant.

Keywords

Attention-deficit/hyperactivity disorder (ADHD); traumatic brain injury (TBI); functional near-infrared spectroscopy (fNIRS); continuous performance task (CPT); one-way analysis of variance (one-way ANOVA); one-way analysis of covariance (one-way ANCOVA).

Introduction

Primary attention-deficit/hyperactivity disorder (ADHD) and traumatic brain injury (TBI) are major general public health issues. The prevalence of ADHD among adults is estimated to be between 3 to 4%.[1] People with ADHD cannot focus on tasks for longer periods of time and have trouble organizing their everyday lives.[14] This leads to relationship problems, financial burden on family, themselves, and society, and overall worsening of their quality of life. Those with TBI may have attention problems such as maintaining focus and shifting attention.[11] Every year, 1.5 million TBIs occur in the U.S. for children and adults.[39] The World Health Organization (WHO) estimated that, "by 2020, TBI could become the third largest source of disease and disability in the world, behind heart disease and depression."[28]

Those affected by ADHD are categorized into one of three presentations: combined presentation, predominantly inattentive presentation, and predominantly hyperactive/impulsive presentation.[7] Previous research on ADHD using functional near-infrared spectroscopy (fNIRS) showed that right inferior and middle frontal gyrus were activated in control groups but was absent for children with ADHD.[25] Another study showed that there was altered prefrontal cortex activity measured with fNIRS in children with ADHD compared to children without ADHD.[22,27]

For those affected by TBI, they may experience attention deficits that are related to damages in the frontal region of the brain.[3] However, in a study on TBI-induced secondary ADHD, there is a significant association of secondary ADHD with severity of TBI in children and adolescents, though secondary ADHD is not significantly associated with the lesion area.[24] Another study shows that symptoms of inattention were more stable for adolescents without preinjury ADHD, and that the changes in ADHD symptoms reflected the severity of TBI.[18]

The current study focused on functional brain activation and connectivity among those with ADHD, TBI, and none of the two (normal control, NC) to determine any abnormal activations and significant connectivity differences using fNIRS.

fNIRS is a flexible, low cost, and non-invasive imagining technique that offers high temporal resolution of the human cortex as compared to some other techniques.[21,33] It indirectly measures brain activity by measuring the light intensity changes scattered back after some absorption by oxygenated hemoglobin (HbO) and deoxygenated hemoglobin (HbR). Near-infrared light includes the wavelength from 650 to 1000 nm, and the optical window is around 700 to 900 nm (see **Figure 1**).[10,17] A pairing of two wavelengths, 690 and 830 nm, was chosen as the wavelengths for measuring changes in HbO and HbR induced by cortical activation for functional brain study for its optimal signal-to-noise ratio.[31]

Method

Participants

Fifty-nine young adult subjects, ranging from 18 to 27 years of age, participated in this study. All the participating subjects were recruited from around New Jersey Institute of Technology (NJIT) using study flyers. This study was approved by the institutional review board (IRB) at NJIT, and written informed consent was obtained from each subject.

None of the subjects were excluded from this study. In the end, 20 adults with ADHD, 20 adults with TBI, and 19 control adults were included in the data analysis. All the subjects were right-handed or ambidextrous using Edinburgh Handedness Inventory[29] to minimize neurobiological heterogeneity.[15] Additionally, the groups were balanced for age and gender to minimize neurobiological differences.[13,30] Most of the data have been previously collected. Of the 59 subjects, eight were recruited this summer and were all placed in the ADHD group (see **Table 1**).

Exclusion criteria for both ADHD and TBI are: not right-handedness, not from 18 to 27 years of age, and having been previously diagnosed and have other mental disorders, medical conditions, and learning disabilities. Specifically for ADHD group, the subjects should not have TBI and, for those who take medication, should not be taking non-stimulant medications. As for TBI, those who were rated as severe for Glasgow Coma Scale (GCS) and those who were diagnosed with ADHD prior to the diagnosis of TBI were excluded.

Subjects with history of TBI were evaluated using Glasgow Coma Scale (GCS). Subjects who were determined to have moderate (scale of 9-12) or mild (scale of 13 and above) brain injury in GCS were placed in the TBI group.[40] Other subjects were evaluated using Conners' Adult ADHD Rating Scales (CAARS). Those who received a T-score of greater than 64 for inattention and/or combined sections in CAARS were grouped as ADHD for their inattention symptoms.[6] The control group excluded subjects who had a history of brain injury or diagnosis of ADHD, or a T-score of greater than 64 for inattention and/or combined sections in CAARS.

fNIRS Data Collection

Six regions of interest (ROI) were selected for their role in visual attention processing of the human brain: bilateral middle frontal gyri (MFG), bilateral inferior occipital cortexes (IOC), and bilateral calcarine gyri (CG).[9,25]

To map head location landmarks onto a human brain template for each subject, Brainsight machine was used (see **Figure 2**).[4] Brainsight positioning camera determined locations for nasion, bilateral pre-auricular points, head sample landmarks, approximated ROI locations, and source, detector, and channel locations. Nasion, bilateral pre-auricular points, and head landmark samples were used to determine head sizes for subjects.

Cw6 fNIRS continuous wave (CW) machine was used to measure the concentration changes of HbO and HbR[10] with a sampling frequency of 50 Hz. Both HbO and HbR were collected, but HbO was used as the chromophore of interest because it has a better signal-to-noise ratio as compared with that of HbR.[34] Further discussion does not include HbR.

To measure the ROIs with the Cw6 device, three custom-made head cap straps[41] were placed in the approximated ROI locations provided by Brainsight on the subjects' heads. A schematic of sources, detectors, and channels is shown in **Figure 3**. A total of 8 near-infrared light (NIR) sources, 16 NIR detectors, and 24 channels were used. To minimize light attenuation, hair was moved away from the sources and detectors.[21] Sources and detectors were marked for each ROI, and the channels were determined by measuring between the source-detector pairs. The channels were chosen in this manner because of the path that the NIR light takes (see **Figure 4**).

The device used to perform the experiment was a Lenovo laptop with the task program installed. The program used to determine the activation amplitude of the six ROIs and the connectivities between each ROI was MATLAB[23]. The associated toolboxes used were: HOMER2[12], NIRS_SPMv4[16,19,35,37,43], and BrainNet Viewer[42]. HOMER2 provided the functionality for bandpass filter and the modified Beer-Lambert Law; NIRS_SPMv4 provided the functionality for generation of significant amplitude magnitude change maps; and BrainNet Viewer provided the functionality for mapping connectivities between the ROIs.

Experimental Task for fNIRS Data Collection

Each of the groups underwent the continuous performance task (CPT). CPT was used because it was previously used for collecting data and because of its role in testing visual attention processing. The CPT is based on the visual sustained attention task.[20] A detailed picture of the task is shown in **Figure 5**. This task's duration was five minutes, with alternating 30-second periods of rest (R) and task (T) at a frequency of 0.0167 Hz. To minimize distractions and NIR light exposure to eyes, the room was darkened and all phones were silenced, and the head caps were covered with a black cloth, respectively. The subjects were asked to avoid speaking/making sound and to minimize their facial expressions as these facial movements can create noticeable noises.[2]

During the resting stage, subjects were asked to relax and look blankly at the screen. The start of the task period was denoted by a red crosshair that appears on the center of the screen. A series of 3-set numbers followed. Each set of numbers were shown in 1.2s, and time break between each set was 1.8s. A total of 10 set of numbers were shown in each task period. The subjects were asked to memorize the first three set; the set was also differentiated from the other sets by using red numbers to help mark the target set to remember. For the nine sets following the red set, the subjects were asked to mark them as either matching the first red set (both numbers and the sequence they are in) or not matching. Matching was marked by a left mouse button click, and not matching was marked by a right mouse button click. Responses of less than 75% accuracy were discarded; accuracy has a significant effect on testing attentional networks.[8]

The total task time for CPT that the subjects had completed was 10 minutes, which corresponds to two CPTs. The recorded data time was longer to avoid missing out on any of the task time. Additional time were spent on setting up and calibrating head cap, practice runs, and additional paperwork. Normally, the total experiment time ranged from 60 to 90 minutes.

Individual and Group Image Processing

To process the data, each groups' files were organized in a particular way. A custom MATLAB program was used to standardize the naming conventions of each file. There were two additional subroutines: one pre-processed the individual *.nirs* data, and the other renamed the *.nirs* data files as either run01 (first run of CPT) or run02 (second run of CPT).

The data collected in the *.nirs* file is light intensity change matrix of the 24 channels over time. The individual processing subroutine removed extraneous time down to 5 minutes with the help of a trigger set at the start of the program. The recorded time before the trigger and after 5 minutes since trigger was removed as extra time.

After removal of extraneous time, the data was bandpassed to select the frequency range of interest and converted from light intensity change to HbO concentration change using Butterworth filter.[32] Light intensities were converted to optical density changes using the optical density formula. Bandpass filter with passband of 0.01 to 0.15 Hz was used as previous studies showed this range includes gross excitation of the brain and resting brain activation level.[38] The optical density matrix was low-pass filtered using 0.15 to filter out physiological signals like the cardiac component and respiratory component.[34] A high-pass filter of 0.01 was used to preserve the experimental signal (0.0167 Hz). The high-pass filter also removed very low frequency blood oscillations. After bandpassing the optical density signal, optical density changes were converted to concentration changes of HbO using the Modified Beer-Lambert Law[21] shown in **Equation 1**. In the equation, the change in optical density (analogous to light attenuation) is ΔA, specific absorption coefficient is α, change in concentration of chromophore is Δc, distance between source and detector is L, and the path traveled by IR light is differential pathlength factor (DPF).

The processing of the pre-processed data underwent three main steps to obtain the finalized activation mapping of the ROIs. The steps were: detrending of HbO

concentration changes, generalized linear modelling, and mapping of significant activation. In detrending, discrete wavelet transform with Minimal Description Length Principle (Wavelet-MDL) was utilized. This part of processing turned the concentration change signal into mutually orthogonal wavelets, and MDL minimized the number of wavelets created to decrease the number of variables. Decreasing the number of variables removes the global trends to help with the next step: Generalized Linear Modeling (GLM).

GLM is a regression model used to obtain the amplitude changes from concentration changes.[26,36] The formula can be condensed into what is shown in **Equation 2**. In the equation, Y is the measured concentration change matrix, X is the model matrix with various variables, β is the amplitude change matrix of the variables in the model, and ε is the uncorrected error component matrix.

Before arriving at the data processing step, the noise component outside the passband was removed. Furthermore, the signal processing step using Wavelet-MDL minimizes the number of variables in the model matrix and removing the global trends. However, there were still unknown errors that needed to be minimized.

To achieve a better result, pre-coloring was used in conjunction with GLM. Pre-coloring applied a transformation matrix S to each of the terms (see **Equation 3**).[26] The remaining error terms were further described by $\Sigma\varepsilon$, where Σ is the unknown error terms and ε is the known error term that is identically distributed $\sim N(0, \sigma^2 I)$. The S transformation matrix should be robust enough to remove the Σ term, leaving only the ε term behind that is identically distributed $\sim N(0, \sigma^2 S^T)$. Although this can lower the power efficiency of getting a better β matrix, pre-coloring made the remaining error terms easily distinguishable. After pre-coloring, the parameters were implemented into GLM to isolate β matrix, which can be mapped to the cortical ROIs.

The coordinates were mapped to a brain template created by averaging 159 subjects for an average brain size.[16,19,35,37,43] Afterwards, the amplitude data (β) was combined with the ROI coordinate data. The last step of mapping used one-sample t-test to show the regions where there were significant amplitude changes that corresponded to activation changes. A p-value of 0.05 was used for the significance. A Gaussian random function (GRF) was used to map the β values collected at the end of GLM and pre-coloring. P-values of less than 0.05 corresponded to voxels with significant different values from the mean which pointed to significant activations.

Statistical Analysis of Processed Data

Distributions of population activation magnitudes of ROI and between-ROI connectivities were assumed to be normally distributed. To determine significance in activation magnitudes of ROI and between-ROI connectivities, one-sample t-test, one-way analysis of variance (one-way ANOVA), and one-way analysis of covariance (one-way ANCOVA) were used. Within-group significant ROI activations and between-ROI connectivities were determined by using one-sample t-test with the average ROI activation across groups and between-ROI connectivities as the test values, respectively.

To compare among the three groups, one-way ANOVA was used; Tukey Honestly Significant Difference (Tukey-HSD) was used to determine pairwise differences.

Results

Demographics

Demographic measures for age and gender did not show a significant difference among the three groups. Chi-square test did not show a significant difference for gender among the groups with a p-value of 0.992. One-way ANOVA did not show a significant difference for age among the groups with a p-value of 0.362.

ROI Significant Brain Activations

All ROIs are significantly activated in each of the three groups (see **Figure 6** and **Table 2**). One-way ANOVA shows that there is a significant difference among the groups for right CG. After performing Tukey-HSD, there is a significant difference between groups TBI and NC with TBI having an increased activation in the right CG as compared to activation for NC. After regressing out the covariates, including gender and age, one-way ANCOVA also shows that there is a marginally significant difference among the groups for right CG. After performing Tukey-HSD, there is also the same significant difference found in one-way ANOVA. Age and gender were not the significant factors in determining group differences. Group factor was marginally significant in determining group differences.

Between-ROI Significant Brain Connectivities

There are some significant connectivities within each of the three groups (see **Figure 7** and **Table 3**). One-way ANOVA shows that there are significant differences between left MFG and right CG, left CG and right IOC, and right CG and right IOC among the three groups. After performing Tukey-HSD, there are significant differences between: NC and TBI groups with TBI having a decreased connectivity compared to that of NC's for connectivity between left MFG and right CG, ADHD and NC groups with ADHD having an increased connectivity compared to that of NC's for connectivity between left CG and right IOC, and TBI and NC groups with TBI having an increased connectivity compared to that of NC's for connectivity between right CG and right IOC. After regressing out the covariates, One-way ANCOVA also shows the same significant differences found in one-way ANOVA. After performing Tukey-HSD, there are also the same significant differences found in one-way ANOVA. Additionally, a significant difference between ADHD and TBI group was found with ADHD having a higher connectivity as compared to that of TBI's for connectivity between left MFG and right CG. Age and gender were not significant factors in determining connectivity differences; group differences significantly accounted for the connectivity differences**.**

Conclusion

The current data suggests there are abnormal brain activation in right CG and significantly increased connectivities between left MFG and right CG, and right CG and right IOC among the three groups. Brain activation in right CG, connectivity between left MFG and right CG, and connectivity between right CG and right IOC may play a role for

inattention in young adults with TBI. Connectivity between left MFG and right CG may play a role for inattention in young adults with primary ADHD.

In this study, age and gender did not have a significant effect on the brain activation of the right CG and did have an effect on the functional connectivity between left MFG and right CG, albeit insignificant.

Future Works

Future works for continuing this research are to increase statistical power by recruiting more subjects and to use multimodal magnetic resonance imaging (MRI) technique (functional MRI, structural MRI, Diffusion Tensor Imaging) in conjunction with the current fNIRS data.

Acknowledgments

This research experience for undergraduates at NJIT was funded by NSF. This study was conducted in the Computational Neuroanatomy and Neuroinformatics Lab under Dr. Xiaobo Li. I would like to acknowledge Dr. Khreishah, Dr. Misra, and Dr. Li for this research experience. I would like to acknowledge the contributions of my student mentor, Ziyan Wu, for providing some resources for literature review and peer editing this paper. I would also like to acknowledge the contributions of Yuyang Luo for his help with statistical analysis and Akshaya Kirithy Baskar for her help in recruiting and screening participants for the study.

References

1. Attention deficit hyperactivity disorder: diagnosis and management of ADHD in children, young people and adults. (2009). Leicester: British Psychological Society.
2. Balardin, J. B., Morais, G. A., Furucho, R. A., Trambaiolli, L. R., & Sato, J. R. (2017). Impact of communicative head movements on the quality of functional near-infrared spectroscopy signals: negligible effects for affirmative and negative gestures and consistent artifacts related to raising eyebrows. Journal of Biomedical Optics, 22(4), 046010. doi:10.1117/1.jbo.22.4.046010.
3. Bigler, E. D. (2007). Anterior and middle cranial fossa in traumatic brain injury: Relevant neuroanatomy and neuropathology in the study of neuropsychological outcome. Neuropsychology, 21(5), 515-531. doi:10.1037/0894-4105.21.5.515.
4. Brainsight NIRS User Manual v2.3. (2015). Rogue Research Inc. Retrieved June 10, 2017, from https://www.rogue-research.com/nirs/.
5. Cerebral oxygenation (Monitoring and imaging) Part 2. (n.d.). Retrieved July 08, 2017, from http://what-when-how.com/neuroanaesthesia-and-neurointensive-care/cerebral-oxygenation-monitoring-and-imaging-part-2/.
6. Conners, C.K., et al., Conner's Adult ADHD Rating Scales (CAARSTM) - Technical Manual. 1999, Multi-Health Systems; North Tonawanda, NY.
7. Diagnosis of ADHD using DSM-5TM. (n.d.). Retrieved August 01, 2017, from http://adhd-institute.com/assessment-diagnosis/diagnosis/dsm-5/.
8. Fan, J., Gu, X., Guise, K. G., Liu, X., Fossella, J., Wang, H., & Posner, M. I. (2009). Testing the behavioral interaction and integration of attentional networks. Brain and Cognition, 70(2), 209-220. doi:10.1016/j.bandc.2009.02.002.
9. Fan, J., Mccandliss, B. D., Sommer, T., Raz, A., & Posner, M. I. (2002). Testing the Efficiency and Independence of Attentional Networks. Journal of Cognitive Neuroscience, 14(3), 340-347. doi:10.1162/089892902317361886.
10. Ferrari, M., & Quaresima, V. (2012). A brief review on the history of human functional near-infrared spectroscopy (fNIRS) development and fields of application. NeuroImage, 63(2), 921-935. doi:10.1016/j.neuroimage.2012.03.049.
11. Graver, C. J. (n.d.). Evaluating Attention Deficits in Brain Injury with the T.O.V.A. (Tech.). Retrieved July 30, 2017, from http://www.tovatest.com/downloads/Evaluating_Attention_Deficits_in_Brain_Injury_with_theTOVA.pdf.
12. HOMER2. (n.d.). Retrieved June 20, 2017, from http://homer-fnirs.org/.
13. Ingalhalikar, M., Smith, A., Parker, D., Satterthwaite, T. D., Elliott, M. A., Ruparel, K., . . . Verma, R. (2013). Sex differences in the structural connectome of the human brain. Proceedings of the National Academy of Sciences, 111(2), 823-828. doi:10.1073/pnas.1316909110.
14. Jang, H., Lee, J. Y., Lee, K. I., & Park, K. M. (2017). Are there differences in brain morphology according to handedness? Brain and Behavior, 7(7). doi:10.1002/brb3.730.
15. Jang, K. E., Tak, S., Jung, J., Jang, J., Jeong, Y., and Ye, J. C., 2009, Wavelet-MDL detrending for near-infrared spectroscopy (NIRS),” Journal of Biomedical Optics, vol. 14, no. 3, pp. 1-13.
16. Institute for Quality and Efficiency in Health Care. (2015). Attention deficit hyperactivity disorder (ADHD): ADHD in adults. Retrieved June 11, 2017, from https://www.ncbi.nlm.nih.gov/pubmedhealth/PMH0079161/.

17. Kumar, V., Shivakumar, V., Chhabra, H., Bose, A., Venkatasubramanian, G., & Gangadhar, B. N. (2017). Functional near infra-red spectroscopy (fNIRS) in schizophrenia: A review. Asian Journal of Psychiatry, 27, 18-31. doi:10.1016/j.ajp.2017.02.009.
18. Levin, H., Hanten, G., Max, J., Li, X., Swank, P., Ewing-Cobbs, L., . . . Schachar, R. (2007). Symptoms of Attention-Deficit/Hyperactivity Disorder Following Traumatic Brain Injury in Children. Journal of Developmental & Behavioral Pediatrics, 28(2), 108-118. doi:10.1097/01.dbp.0000267559.26576.cd.
19. Li, H., Tak, S., and Ye, J.C., 2012. Lipschitz Killing curvature based expected Euler characteristics for p-value correction in fNIRS. J. Neurosci. Meth. 204, 61-67.
20. Li, X., Sroubek, A., Kelly, M. S., Lesser, I., Sussman, E., He, Y., . . . Foxe, J. J. (2012). Atypical Pulvinar–Cortical Pathways During Sustained Attention Performance in Children With Attention-Deficit/Hyperactivity Disorder. Journal of the American Academy of Child & Adolescent Psychiatry, 51(11). doi:10.1016/j.jaac.2012.08.013.
21. Lloyd-Fox, S., Blasi, A., & Elwell, C. (2010). Illuminating the developing brain: The past, present and future of functional near infrared spectroscopy. Neuroscience & Biobehavioral Reviews, 34(3), 269-284. doi:10.1016/j.neubiorev.2009.07.008).
22. Marx, A., Ehlis, A., Furdea, A., Holtmann, M., Banaschewski, T., Brandeis, D., . . . Strehl, U. (2015). Near-infrared spectroscopy (NIRS) neurofeedback as a treatment for children with attention deficit hyperactivity disorder (ADHD)–a pilot study. Frontiers in Human Neuroscience, 8. doi:10.3389/fnhum.2014.01038.
23. MATLAB. (n.d.). Retrieved June 10, 2017, from https://www.mathworks.com/products/matlab.html.
24. Max, J., Lansing, A., Koele, S., Castillo, C., Bokura, H., Schachar, R., . . . Williams, K. (2004). Attention Deficit Hyperactivity Disorder in Children and Adolescents Following Traumatic Brain Injury. Developmental Neuropsychology, 25(1), 159-177. doi:10.1207/s15326942dn2501&2_9.
25. Monden, Y., Dan, I., Nagashima, M., Dan, H., Uga, M., Ikeda, T., . . . Yamagata, T. (2015). Individual classification of ADHD children by right prefrontal hemodynamic responses during a go/no-go task as assessed by fNIRS. NeuroImage: Clinical, 9, 1-12. doi:10.1016/j.nicl.2015.06.011.
26. Monti, M. (2011). Statistical Analysis of fMRI Time-Series: A Critical Review of the GLM Approach. Frontiers in Human Neuroscience, 5. doi:10.3389/fnhum.2011.00028.
27. New study supports link between ADHD and traumatic brain injury. (2015, August 23). MedicalNewsToday. Retrieved August 02, 2017, from http://www.medicalnewstoday.com/articles/298478.php.
28. Negoro, H., Sawada, M., Iida, J., Ota, T., Tanaka, S., & Kishimoto, T. (2009). Prefrontal Dysfunction in Attention-Deficit/Hyperactivity Disorder as Measured by Near-Infrared Spectroscopy. Child Psychiatry & Human Development, 41(2), 193-203. doi:10.1007/s10578-009-0160-y.
29. Oldfield, R.C., The assessment and analysis of handedness: the Edinburgh inventory. Neuropsychologia, 1971. 9(1): p. 97-113.
30. Peters, R. (2006). Ageing and the brain. Postgraduate Medical Journal, 82(964), 84–88. http://doi.org/10.1136/pgmj.2005.036665.

31. Sato, H., Kiguchi, M., Kawaguchi, F., & Maki, A. (2004). Practicality of wavelength selection to improve signal-to-noise ratio in near-infrared spectroscopy. NeuroImage, 21(4), 1554-1562. doi:10.1016/j.neuroimage.2003.12.017.
32. Scarpa, F., Cutini, S., Scatturin, P., Dell'Acqua, R., & Sparacino, G. (2010). Bayesian filtering of human brain hemodynamic activity elicited by visual short-term maintenance recorded through functional near-infrared spectroscopy (fNIRS). Optics Express, 18(25), 26550. doi:10.1364/oe.18.026550.
33. Sorger, B. (2017) Functional Near-Infrared Spectroscopy (fNIRS): A promising BCI technique. Retrieved from https://www.slideshare.net/InsideScientific/fnirs-and-brain-computer-interface-for-communication.
34. Strangman, G., Franceschini, M. A., & Boas, D. A. (2003). Factors affecting the accuracy of near-infrared spectroscopy concentration calculations for focal changes in oxygenation parameters. NeuroImage, 18(4), 865-879. doi:10.1016/s1053-8119(03)00021-1.
35. Tak, S., Jang, J., Lee, K., and Ye, J. C., 2010, Quantification of CMRO2 without hypercapnia using simultaneous near-infrared spectroscopy and fMRI measurements. Physics. Med. Biol. 55, 3249-3269.
36. Tak, S., Jang, K. E., Jung, J., Jang, J., Jeong, Y., & Ye, J. C. (2008). NIRS-SPM: statistical parametric mapping for near infrared spectroscopy. Multimodal Biomedical Imaging III. doi:10.1117/12.762291.
37. Tak, S., Yoon, S. J., Jang, J. Yoo, K., Jeong, Y., and Ye, J. C., 2011, Quantitative analysis of hemodynamic and metabolic changes in subcortical vascular dementia using simultaneous near-infrared spectroscopy and fMRI measurements. NeuroImage 55, 176-184.
38. Tong, Y., Hocke, L. M., Licata, S. C., & Frederick, B. D. (2012). Low-frequency oscillations measured in the periphery with near-infrared spectroscopy are strongly correlated with blood oxygen level-dependent functional magnetic resonance imaging signals. Journal of Biomedical Optics, 17(10), 1060041. doi:10.1117/1.jbo.17.10.106004.
39. Traumatic Brain Injury & Concussion. (2016, January 22). Retrieved July 30, 2017, from https://www.cdc.gov/traumaticbraininjury/pubs/tbi_report_to_congress.html.
40. Wilson, J. T. (2000). Emotional and cognitive consequences of head injury in relation to the Glasgow outcome scale. Journal of Neurology, Neurosurgery & Psychiatry, 69(2), 204-209. doi:10.1136/jnnp.69.2.204.
41. Wu, Z., Luo, Y., Baskar, A., & Li, X. (2017). Testing cortical activation responding to visual attention in young adults with traumatic brain injury – a functional near-infrared spectroscopy pilot study.
42. Xia M, Wang J, He Y (2013) BrainNet Viewer: A Network Visualization Tool for Human Brain Connectomics. PLos ONE 8: e68910.
43. Ye, J. C., Tak, S., Jang, K. E., Jung, J., Jang, J., 2009, NIRS-SPM: Statistical parametric mapping for near-infrared spectroscopy. NeuroImage 44, 428-447.

Figures, Equations, and Tables

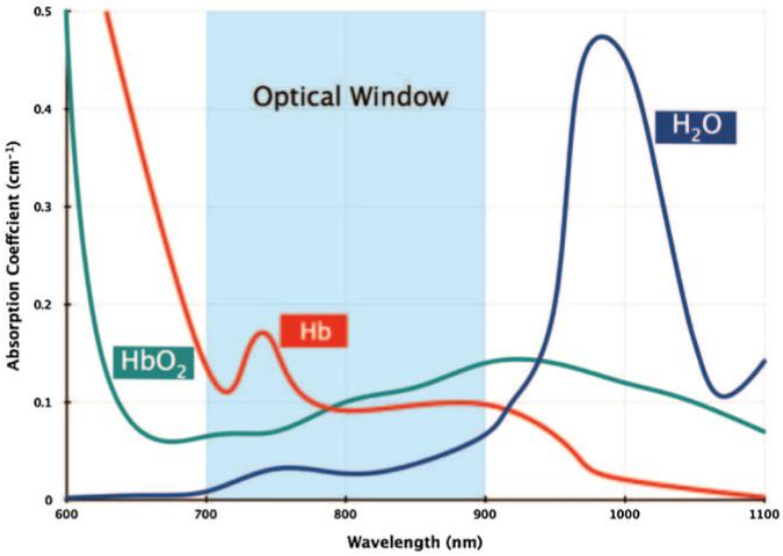

Figure 1. *Optical window for measuring chromophores in near-infrared light wavelength range.*[17]

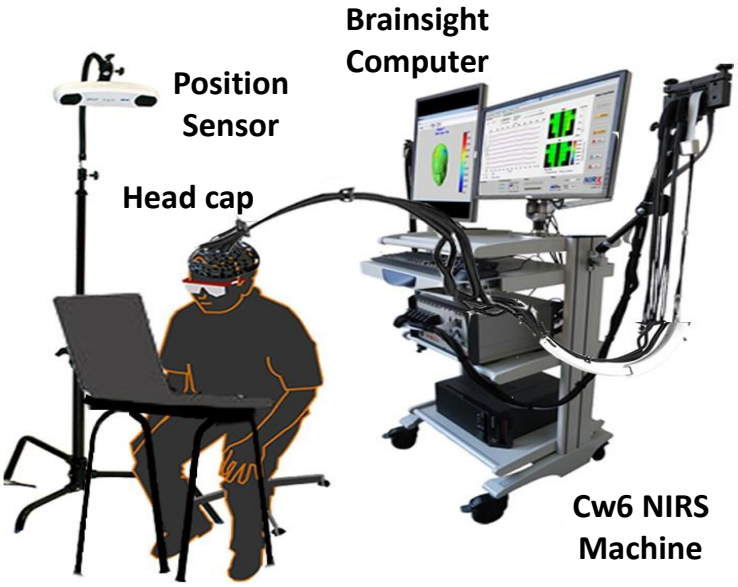

Figure 2. *Data Collection Device Setup.*

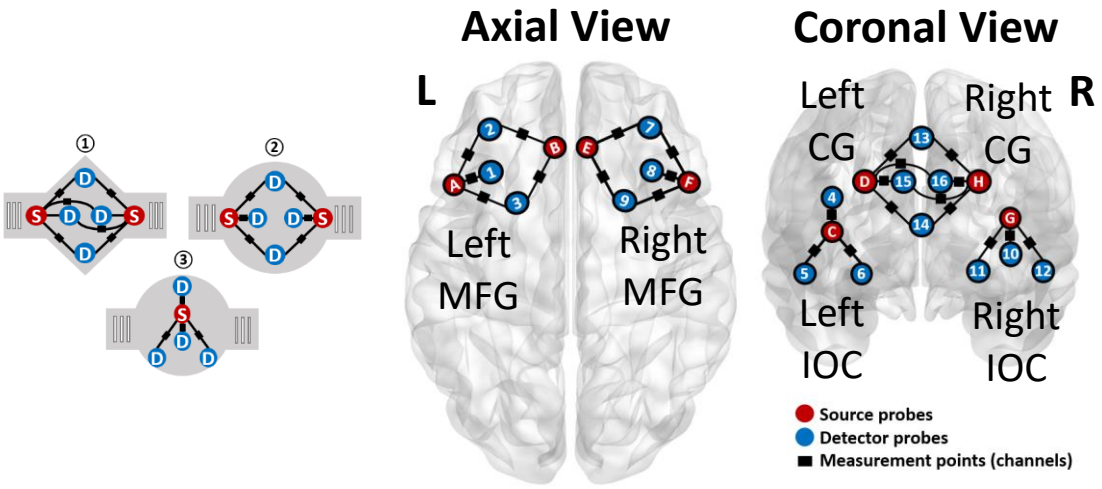

***Figure 3**. Head cap strap design and setup. Sources are designated by red, detectors are designated by blue, and channels are designated by black.*

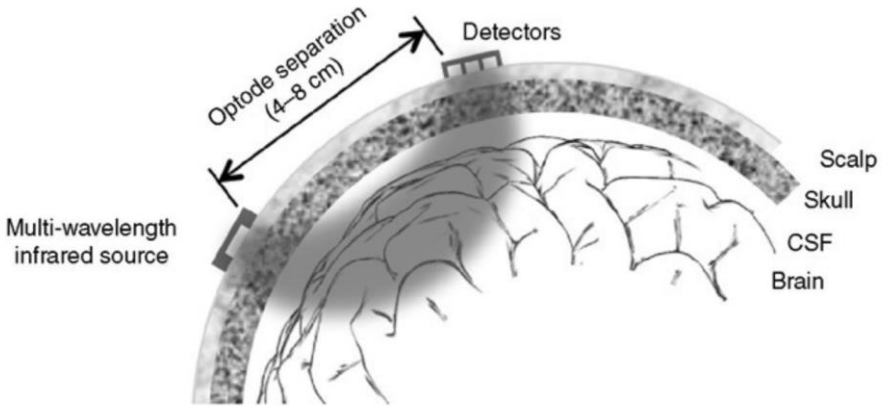

***Figure 4**. Path that NIR light travels in for cortical brain measurements.*[5]

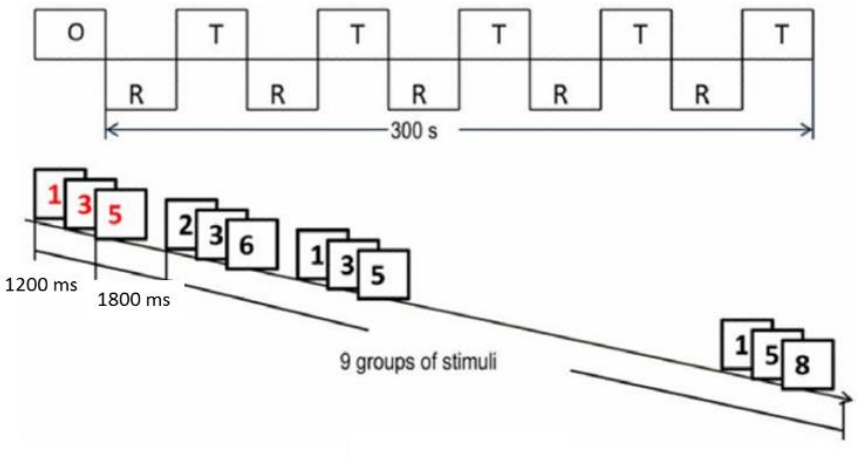

***Figure 5**. Continuous Performance Task.*[20]

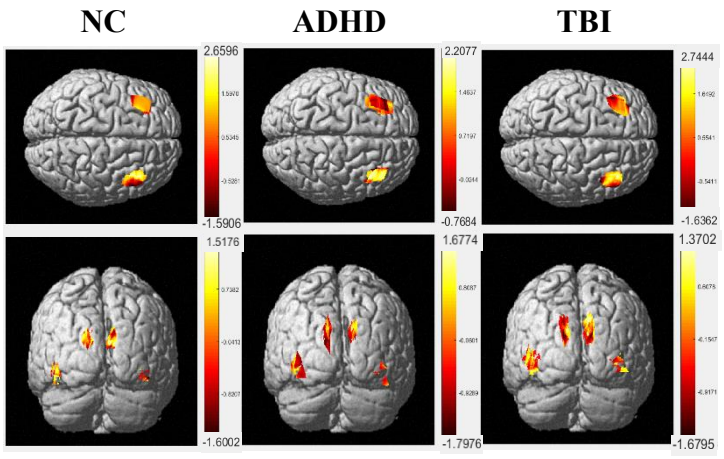

***Figure 6**. Significant concentration amplitude changes in selected ROIs.*

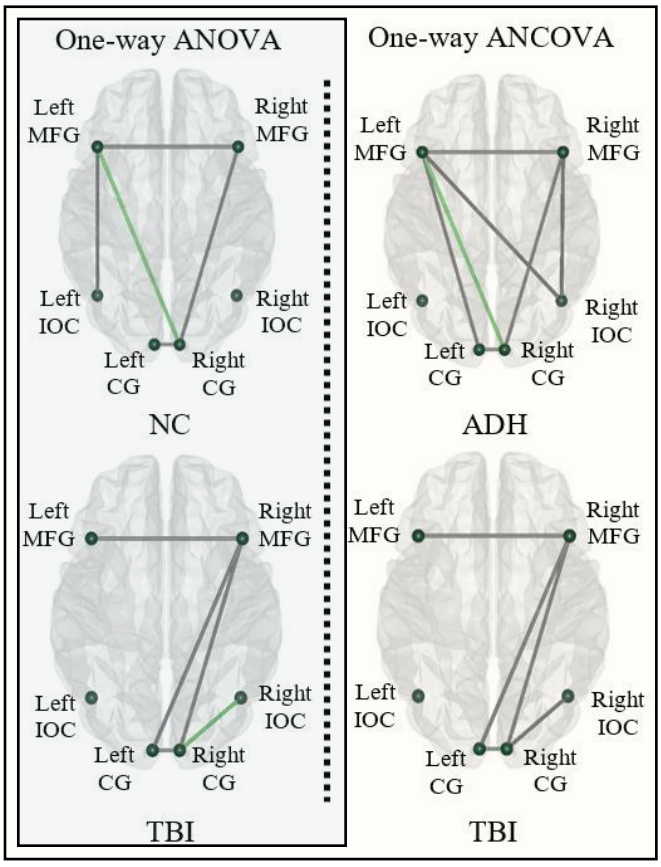

***Figure 7**. Pairwise comparison of significant brain connectivities.*

$$\Delta A = \alpha \cdot \Delta c \cdot L \cdot DPF$$

***Equation 1**. Modified Beer-Lambert Law.*[21]

$$Y = X\beta + \varepsilon$$

***Equation 2**. Generalized Linear Model Approach.*[26,36]

$$SY = SX\beta + S\sum\varepsilon$$

***Equation 3**. Pre-coloring.*[26]

***Table 1**. Demographic measures of the three groups.*

	ADHD = 20		NC = 19		TBI = 20		Sig.
	Mean	SD	Mean	SD	Mean	SD	p-Value
Gender (Male:Female)	14:6		13:6		14:6		$0.992^{\chi 2}$
Age	20.700	2.452	21.053	1.985	20.050	2.164	0.362^{ANOVA}

Abbreviations: ADHD, attention deficit hyperactivity disorder; ANOVA, Analysis of Variance; NC, normal control; SD, standard deviation; Sig., significance value; TBI, traumatic brain injury; Tukey HSD, Tukey Honestly Significant Difference; $\chi 2$, Chi-Square Test

***Table 2**. Differences among groups and covariate significance.*

		Sig.	Post Hoc T-HSD	
	ROIs	p-Value	Groups	p-Value
One-Way ANOVA	Right CG	0.028	TBI > NC	0.027
One-Way ANCOVA	Right CG	0.052	TBI > NC	0.021

Abbreviations: Sig., significance value; T-HSD, Tukey Honestly Significant Difference Post Hoc Test

	F	Sig.
Age	1.180	0.282
Gender	0.276	0.602
Group	3.128	0.052

***Table 3**. Differences among groups and covariate significance.*

	Between-ROI Connectivities	Sig.	Post Hoc T-HSD	
		p-Value	Groups	p-Value
One-Way ANOVA	Left MFG Right CG	0.021	NC > TBI	0.027
	Left CG Right IOC	0.023	ADHD > NC	0.022
	Right CG Right IOC	0.019	TBI > NC	0.014
One-Way ANCOVA	Left MFG Right CG	0.037	ADHD > TBI	0.037
			NC > TBI	0.018
	Left CG Right IOC	0.027	ADHD > NC	0.009
	Right CG Right IOC	0.021	TBI > NC	0.006

left MFG - right CG	F	Sig.	left CG - right IOC	F	Sig.	right CG - right IOC	F	Sig.
Age	1.107	0.297	Age	0.004	0.952	Age	0.141	0.708
Gender	0.967	0.330	Gender	0.972	0.329	Gender	0.002	0.966
Group	3.521	0.037	Group	3.878	0.027	Group	4.169	0.021